The microstructure and elevated temperature strength of tungsten-titanium carbide composite

G. M. SONG
School of Materials Science and Engineering, P.O. Box 433, Harbin Institute of Technology, Harbin 150001, People's Republic of China; Institute of Engineering Mechanics, Harbin 150080, People's Republic of China
E-mail: songguim@hotmail.com

Y. ZHOU, Y. J. WANG
School of Materials Science and Engineering, P.O. Box 433, Harbin Institute of Technology, Harbin 150001, People's Republic of China

A new tungsten matrix composite containing 30 vol% titanium carbide particles (W-TiC) produced by sintering under 20 MPa pressure at 2000°C in a vacuum has been developed in order to improve the elevated temperature strength of tungsten. Flexural strength tests of the W-TiC composite in the temperature range 20–1200°C showed that the strength was significantly increased by the presence of TiC particles. The flexural strength at 1000°C was 1155 MPa, which was much higher than that at 20°C (770 MPa). Microstructural observations showed that a interdiffusion zone was produced at the W matrix-TiC particle interface, and a strong bond was formed between TiC and W, which was very beneficial to the elevated temperature mechanical properties. The mechanisms of fracture at 20°C and 1000°C were investigated. The fracture at 20°C was brittle. There was a growth-coalescence process for the initial cracks during the fracture process of the W-TiC composite at 1000°C, and the W matrix exhibited ductile tearing. The excellent elevated temperature strength of W-TiC composite was attributed to the brittle-ductile transition in the W matrix, which allows more effective strengthening from TiC particles.
© *2002 Kluwer Academic Publishers*

1. Introduction

The research interest in heavy metals has been stimulated by the desire to produce a counterbalance in combustion motors where the working environment temperature is about 1000°C [1]. As a refractory metal with the highest melting point, tungsten is one of the most widely used high temperature materials for its unique combination of good strength, good thermal stability, corrosion resistance and small coefficient of thermal expansion [2–4]. However, the strength of pure W decreases significantly with increasing temperature. For example, the strength at 1000°C decreases ~60% compared with that at room temperature [3], which impedes application as a structural component at high temperatures. Many successful studies on the improvement of the mechanical properties of W by finely dispersed second particles have been reported. For instance, W-ThO₂, W-La₂O₃, W-HfC, W-ZrC, W-TiC, etc. were investigated [5–11]. The particles can restrict tungsten grain growth and dislocation motion, both of which lead to higher strengths and lower creep rates at high temperature. The content of these particles is usually less than 2 vol%. The strength of W however still drastically drops as temperature rises. Tungsten alloys such as W-Ni-Cu and W-Ni-Fe [12–14] possess good mechanical properties, but the lower melting points of nickel, iron and copper usually result in lower high temperature strength in these heavy alloys. So it is necessary to further improve the elevated temperature strength of tungsten to enable wider application in high temperature environments.

Titanium carbide is a refractory ceramic commercially available in particle form with a very high melting temperature, ~3067°C [15]. It has the necessary elevated temperature strength and high Young's modulus required to produce enhanced mechanical properties in tungsten [10]. Furthermore, TiC is compatible with tungsten [16, 17]. W can diffuse into TiC to form a solid solution (Ti, W)C which is beneficial to the strength of TiC [18]. Rapidly increasing demand for high performance materials in recent years has led to the development of metal matrix composites [19]. Up to now, research on tungsten matrix composites reinforced with high content ceramic phase has been rarely reported. In this work, firstly a high volume fraction, 30 vol%, TiC particles are added to a tungsten matrix, and subsequently the effect of TiC particles on the microstructure and elevated temperature strength of the W-TiC composite is reported.

Materials and properties	Tungsten	TiC
Density (g/cm^3)	19.3	4.93
Crystal structure	bcc	fcc
Thermal expansion coefficient ($\times 10^{-6}$ K^{-1})	4.98 (293–1300 K)	7.76 (293–1300 K)
	6.06 (1300–2300 K)	10.4 (1300–2300 K)
Young's modulus (GPa)	385	460–500
Poisson's ratio	0.28	0.25
Melting point (°C)	3410	3067
Strength (MPa)	360–490 (T)	1352 (F)

From [1, 11, 15, 16]. T: tensile strength; F: flexural strength

2. Experimental procedure

Commercial tungsten powder with a mean size of 3.5 μm (purity >99%) and TiC powder with a mean size of 2.5 μm (purity 98% or greater) were used in this study. Fig. 1 shows the shapes of the as-received W and TiC powders. Table I shows the characteristics of tungsten and TiC. W and TiC powders were mixed with ethanol by ball milling for 24 h, and the TiC content was 30 vol%. The slurry was later evaporated and the composite powder was pressed in a steel mold under 200 MPa, and then hot pressed in a graphite mold at 2000°C under 20 MPa pressure in a vacuum of 1.3×10^{-3} Pa for 60 min. For comparisan with the W-TiC composite, pure tungsten was also fabricated using the same procedure.

Flexural strength testing was performed using three-point bending and the specimen size was $2.5 \times 4 \times 30$ mm^3. The crosshead speed was 0.5 mm/min and the span was 20 mm. All the tensile surfaces of the specimens were polished using diamond pastes and the edges were chamfered. The strength was measured from room temperature to 1200°C in an argon atmosphere. Some of the room temperature and high temperature tests were interrupted before failure in order to study the fracture characteristics of the W-TiC composite.

Fracture toughness was evaluated by the single-edge notched beam test with a 16 mm span and a crosshead speed of 0.05 mm/min using test bars of $2 \times 4 \times 20$ mm^3 with a notch of 2 mm in depth and 0.2 mm in width. The specimens having dimensions $1.2 \times 3.5 \times 65$ mm^3 were used for the tests of the elastic modulus at 20°C and 1000°C by the acoustic resonance method in a furnace in an argon atmosphere. The Vickers hardness was tested with a Vickers microhardness tester with the conditions of load of 198 N and duration of 15 s. The densities of the specimens were measured by the Archimedes water-immersion technique.

The microstructure and the fracture characteristics of the W-TiC composite were examined using a scanning electron microscope (SEM). Transmission electron microscopy (TEM) samples were prepared by dimpling and subsequent ion-beam thinning. The microstructure and chemical composition of the composites were investigated using selected area diffraction (SAD) and energy dispersive X-ray spectroscopy (EDS). Crystal phases for pure W and W-TiC composites were characterized by X-ray diffraction (XRD) analysis with Cu K_α-radiation.

3. Results and discussion
3.1. Microstructure

Fig. 2 shows the results of the XRD analyses of the W-TiC composites before and after hot pressing. The phases in the sample before hot pressing are W, TiC and a little free carbon. In the XRD pattern of the sintered sample, there is no carbon peak. There is free carbon in the TiC raw material, hence the diffraction peak of carbon in the XRD pattern of the mixture of W and TiC. If all the carbon diffuses into TiC or reacts with W during the sintering process, this would account for the disappearance of the diffraction peak. Fig. 3 is a low magnification micrograph of the polished surface of the W-TiC composite showing that the TiC particles are well distributed in the W matrix. The uniformity of the microstructure results in isotropic physical properties of the W-TiC composite.

The microstructures observed by TEM are shown in Fig. 4. The W/TiC interface was clean, and no other phases or interface precipitates were observed in the microstructure of the W-TiC composite. TiC particles exist at the W grain boundaries or grain corners, and no TiC particles exist inside the W grains.

In order to determine the chemical composition at the interface, TEM/EDS analyses were conducted at various locations. Fig. 5 shows TEM/EDS concentration
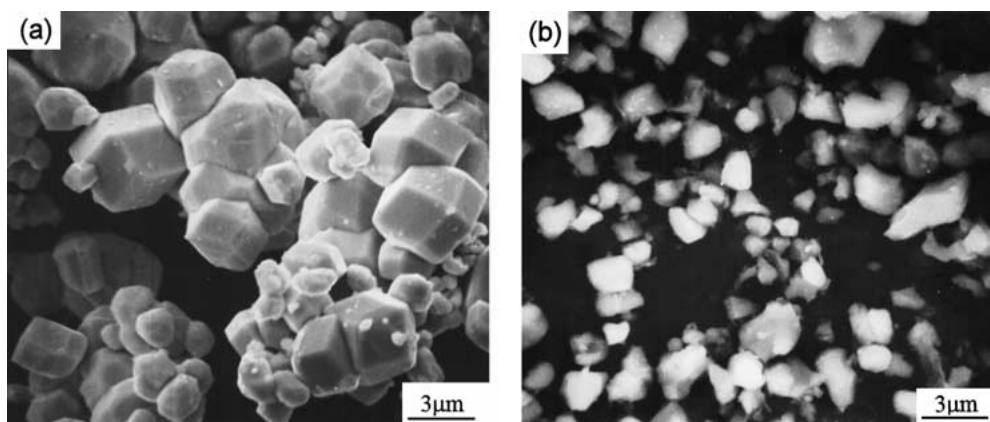

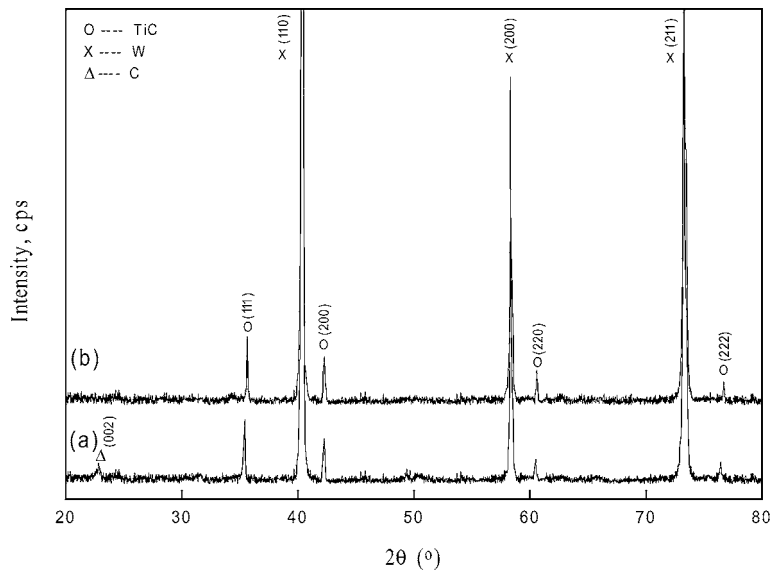*Figure 1* The as-received (a) W and (b) TiC powders.

Figure 2 X-ray diffraction patterns of W-TiC composite (a) before hot-pressing, (b) after hot pressing.
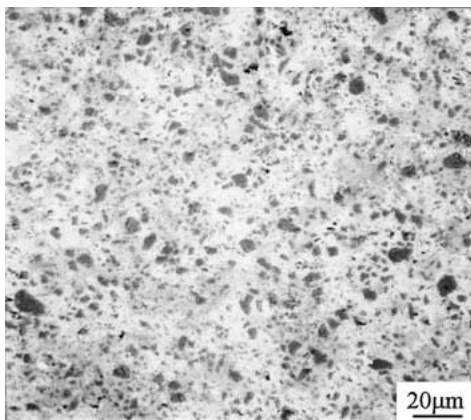

Figure 3 The polished surface of a W-TiC composite specimen, showing a uniform distribution of TiC particles in W matrix.

profiles of Ti and W across the particle-matrix interface zone in the composite. These demonstrate that there was interdiffusion at the W/TiC interface with penetration of W into TiC at the sintering temperature leading to the formation of a solid solution transition zone identified as (Ti, W)C, while a little Ti also diffused into the W. At high temperatures, free carbon from the TiC particles can react with Ti and W, respectively, and the corresponding reactions are as follows [22]:

$$W + C = WC \tag{1}$$

$$2W + C = W_2C \tag{2}$$

$$Ti + C = TiC \tag{3}$$

The free energies of the above three carbides under standard conditions at various temperatures are shown
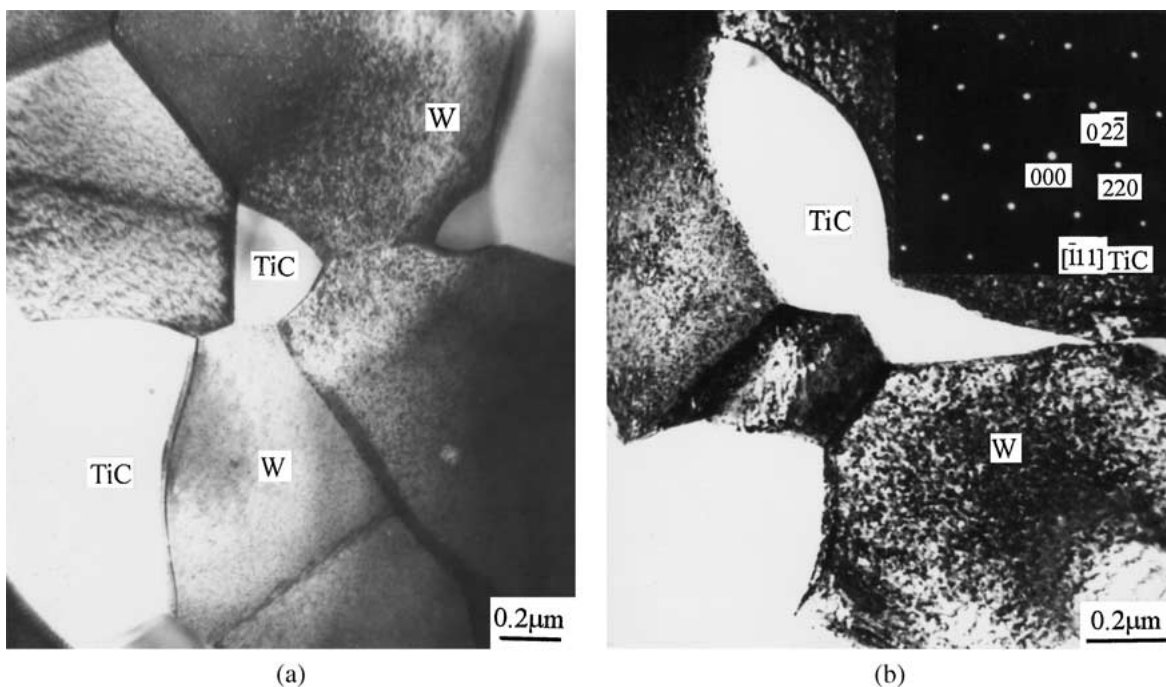

Figure 4 Transmission electron micrographs of the microstructure of the W-TiC composite showing a clean W/TiC interface and no reaction zone formed at the interface: (a) micrograph of W-TiC; (b) micrograph of W-TiC and selected area diffraction pattern of TiC with zone axis [ī11].
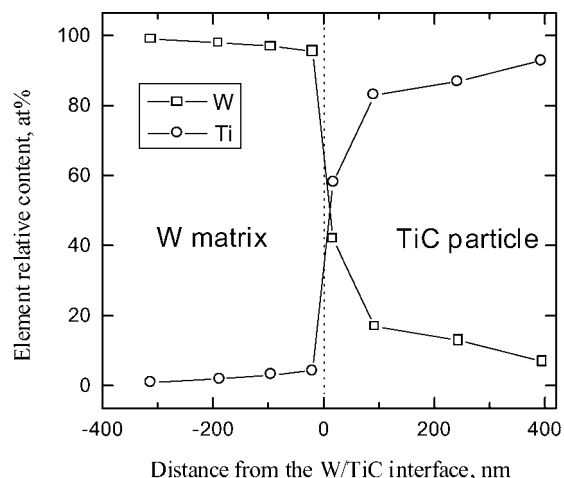
Figure 5 EDS relative concentration profiles of W and Ti at the W/TiC interface in W-TiC composite.
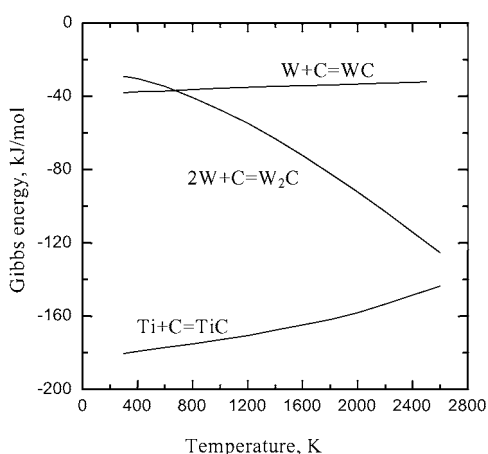

Figure 6 The free energies formation of WC, WC and TiC at various temperatures.

free energy of formation of TiC than W_2C, it is suggested that the remnant free carbon diffused into the nonstoichiometric $(Ti, W)C_{1-x}$ solid solution to replenish the C instead of reacting with W, resulting in a strong interfacial bond.

Preparing fully dense tungsten is difficult without any sintering aids or sintering activators such as Pt, Ni, Pd, [25]. The eutectic temperature of W-TiC is $\sim 2750°C$ according to the phase diagram [26], which is much lower than the melting point of pure W ($3410°C$) [3]. Therefore W/TiC interface sintering should be much faster than the sintering of W grains, resulting in a higher relative density in W-TiC composite (97.0%) compared with pure W material (95.1%). The interdiffusion of W and Ti at the W/TiC interface maybe also promote the densification of the W-TiC composite.

3.2. Mechanical properties

Table II gives the room temperature mechanical properties of the W-TiC composites and pure W materials. Compared with the pure W, the W-TiC composite has a higher relative density although a lower actual density, and a higher hardness, and higher elastic modulus from the direct contribution of TiC particles to the composite. The toughness of the composite is also increased, but, the flexural strength of the composite is slightly decreased.

The flexural strength of the W-TiC composite exhibited an increase over room temperature levels as the test temperature increased from $20°C$ to $1200°C$, as shown in Fig. 7. The highest strength value of 1150 MPa was found at $1000°C$, an increase of 50% compared with the corresponding room temperature strength value of

in Fig. 6. It is evident that these carbides are stable and TiC is the most stable in the temperature range ($20–2400°C$). In the solid phase sintering temperature range ($1500–2000°C$), the remnant free carbon in TiC powders maybe react with W, and the main products should be WC or W_2C, but no W_2C or WC could be observed in the W-TiC composite.

In this study, the starting material TiC_{1-x} is a nonstoichiometric compound with a structural formula of $TiC_{0.96}$ and a NaCl-type structure [23]. Ti^{4+} has a radius of 0.068 nm, and W^{4+} has a radius of 0.070 nm [24]. When W is mixed with TiC and subjected to a high temperature, solid state diffusion takes place, W^{4+} can replace Ti^{4+} in TiC_{1-x} and $(Ti, W)C_{1-x}$ is formed resulting in a decrease in the relative C atom content. Due to the very low content of free carbon, and lower
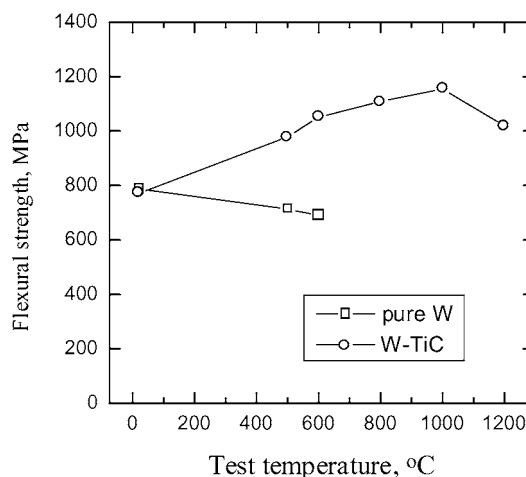

Figure 7 The flexural strength of W-TiC composites and pure W materials as a function of test temperature.

TABLE II The mechanical properties of W-TiC composite and pure W material tested at room temperature

	Density (g/cm^3)	Relative density (%)	Hardness (GPa)	Elastic modulus (Gpa)	Flexural strength (MPa)	Fracture toughness (MPa·m$^{1/2}$)
W-TiC	14.50	97.0	5.77	380	770	8.71
Pure W	18.31	95.1	3.4	313	787	7.61

770 MPa. Strength decreased with further increases in test temperature from 1000°C to 1200°C, but the strength value at 1200°C was 1020 MPa, which is still higher than the room temperature value. The strength of the pure W always decreased with increasing temperature. The specimen of pure W broke without plastic deformation at 600°C but bent without fracture a 800°C, even though the specimen contained a crack, which implies that the pure W has good ductility above 800°C, therefore, 800°C is above the ductile-brittle transition temperature (DBTT) of the pure W.

The elastic modulus values of W-TiC composites and pure W materials were measured by the acoustic resonance method at 20°C (see Table II) and 1000°C, The values for the composites and pure W at 1000°C are 337 GPa and 195 GPa, respectively. The modulus of the composites is significantly higher than that of pure W at both 20°C and 1000°C. Based on the elastic moduli at elevated temperature, W-TiC composites should have good structural stability at elevated temperature.

3.3. Fracture characterization

A fuller understanding of the factors controlling the flexural strength of these materials requires knowledge of their fracture characteristics and the mechanisms of crack initiation and propagation. The stress-deflection curves of the W-TiC composite at different temperatures are shown in Fig. 8. The results from the test at 20°C shows that there is only elastic deformation in the W-TiC composite before failure, but the curves corresponding to 1000°C and 1200°C show non-linearity before failure, which implies that there is plastic deformation and/or a metastable crack propagation before failure in the composites. The general trend is that the flexural strength increased and the deflection (or strain) increased with increasing test temperature, and a little plastic deformation took place before failure at high temperature.
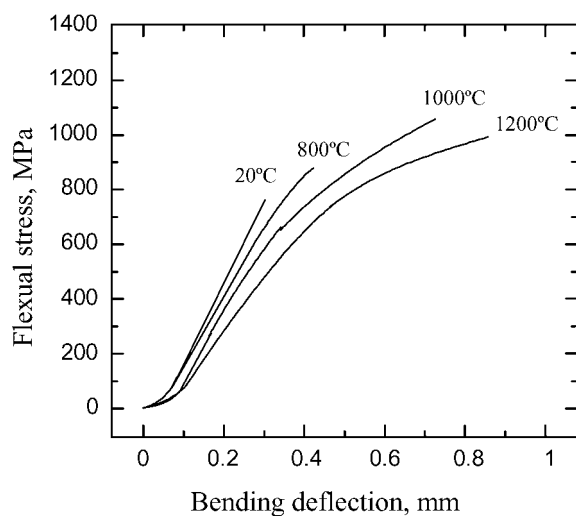

Figure 8 Stress/deflection curves of W-TiC composites at various test temperatures showing a little plastic deformation took place at 1000°C and 1200°C.

Fig. 9 shows the fracture surfaces of W-TiC and pure W specimens tested in bending at various temperatures. Fig. 9a shows the fracture surface of pure W tested at 20°C. As can be seen, the fracture surface exhibits a typical brittle fracture showing regions of intergranular and transgranular fracture. The fracture of pure W at 600°C was intergranular (see Fig. 9b). The morphological features of the fracture surfaces of W matrix in W-TiC composites (see Fig. 9c) tested at 20°C were similar to those of pure W materials (see Fig. 9a). However, the fracture surface is rougher, and additionally, the size of the W grains in the W-TiC composites is significant smaller than in the pure W, which implies that TiC inhibited W grain growth during the sintering process. Crack deflection is an important mechanism in the composite, and it should make a significant contribution to the toughness of the composite.

On the fracture surface of the W-TiC composite tested at 800°C (see Fig. 9d), the W matrix still exhibits a complex mixed fracture mode of intergranular and transgranular fracture. Fine dimples and tear ridges can be found on the fracture surface of W-TiC composite tested at 1000°C (see Fig. 9e), indicating W matrix ductility. The same morphology can also be found on the fracture surfaces of the specimen tested at 1200°C (see Fig. 9f). Ductile tearing of W matrix in the composites at 1000°C and 1200°C contrasts with the pure W material tested at 600°C where no transgranular fracture of the W matrix was found. Thus, the fracture surfaces of W-TiC composite at elevated temperatures were complex mixtures of brittle cleavage of TiC and ductile tearing of W matrix.

Observation of the cracking behavior of the W-TiC specimen tested at 1000°C were performed by interrupting the bending test several times. Under an increasing external stress, a crack usually initiated in the W matrix at a bigger TiC particle or at TiC clusters on the tensile surface (see Fig. 10a). Subsequently, some microcrack zones formed in front of bigger cracks (see Fig. 10b), which led to damage zones ahead of these bigger cracks. The formation of the microcrack zone consumed the strain energy and reduced the effective stress intensity at the crack tip. With further increases in the external stress, the microcracks grew to form discontinuous short cracks of 10~30 μm in length (see Fig. 10c). During the coalescence of these short cracks, ductile tears in the W matrix could be observed (see figures 10d). During the fracture process, ductile teasing of the W matrix and crack deflection occurred (see Fig. 10d–f). Interface cracking was seldom found in this study (see Fig. 10f), indicating that the W/TiC interface bonding strength was higher than the W matrix strength at 1000°C.

When a crack initiates in the W-TiC composite at room temperature, the TiC and W matrix can not effectively prevent the crack from propagating. The composite is prone to catastrophic failure in the presence of flaws (such as microcracks and pores), resulting in brittle fracture and a low strength.

When the temperature exceeds the DBTT of W, the ductility of the W matrix in the composite increases significantly. The deformation and ductile tearing of
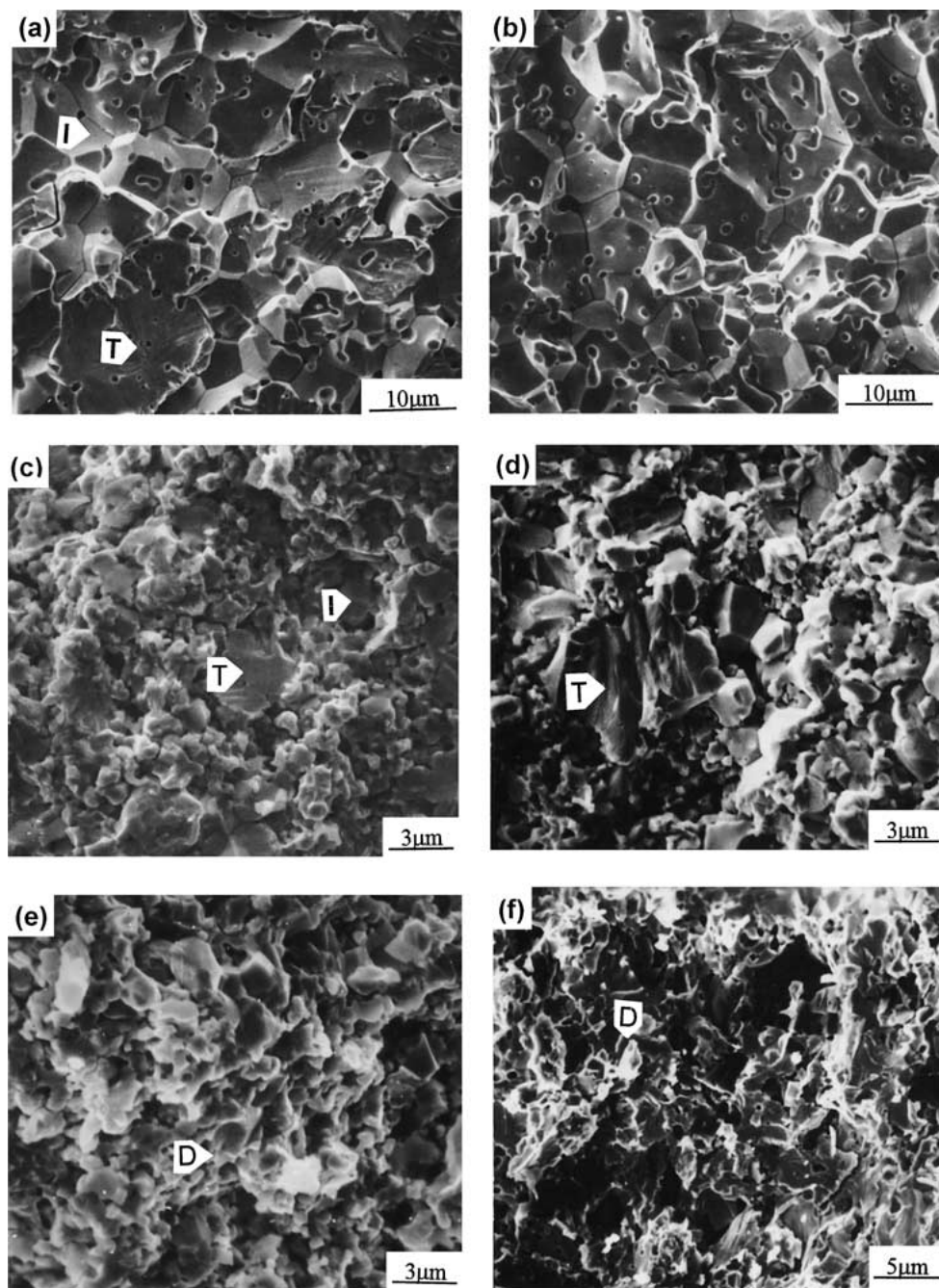
Figure 9 Micrographs of fracture surfaces of W-TiC composite and pure W material tested at various temperatures: (a) pure W, room temperature; (b) pure W, 600°C; (c) W-TiC, room temperature; (d) W-TiC, 800°C; (e) W-TiC, 1000°C; (f) W-TiC, 1200°C, showing transgranular fracture (T), intergranular fracture (I) and fine dimples (D) of W matrix.

the W matrix decrease the crack propagation rate and crack sensitivity, consequently, increasing the damage tolerance of the W-TiC composite at elevated temperature. The metastable crack growth and coalescence in the fracture process result in the corresponding nonlinear stress/deflection curves (see Fig. 8). Furthermore, the hard TiC particles present in the softer W matrix constrained the plastic deformation of the W matrix by hindering dislocation motion, thereby, enhancing the elevated temperature strength of the W-TiC composite.

Fig. 10b reveals that the pure W underwent intergranular fracture at 600°C; however, both transgranular and intergranular fracture are found in the fracture surfacs of the W-TiC composites in the range 800–1200°C. At elevated temperatures, it is important to limit grain boundary sliding in order to attain good elevated tem-

perature strength. Due to the higher strength of the W/TiC interface compared with that of the W grain interior, transgranular fracture of W grains occurs at elevated temperatures, as shown in Fig. 10d–f.

As stated above, the excellent elevated temperature strength of W-TiC composites can be attributed to the brittle-ductile transition in the W matrix, which makes the strengthening effect of TiC more significant at elevated temperatures. Additionally, the following two possible strengthening mechanisms may occur in W-TiC composite at elevated temperature. One is the indirect interaction between dislocations in the ductile W matrix and TiC particles, where the second-phase particles introduce a misfit stress field impeding the movement of dislocations. The other possible strengthening mechanism is particle-hardness effects.
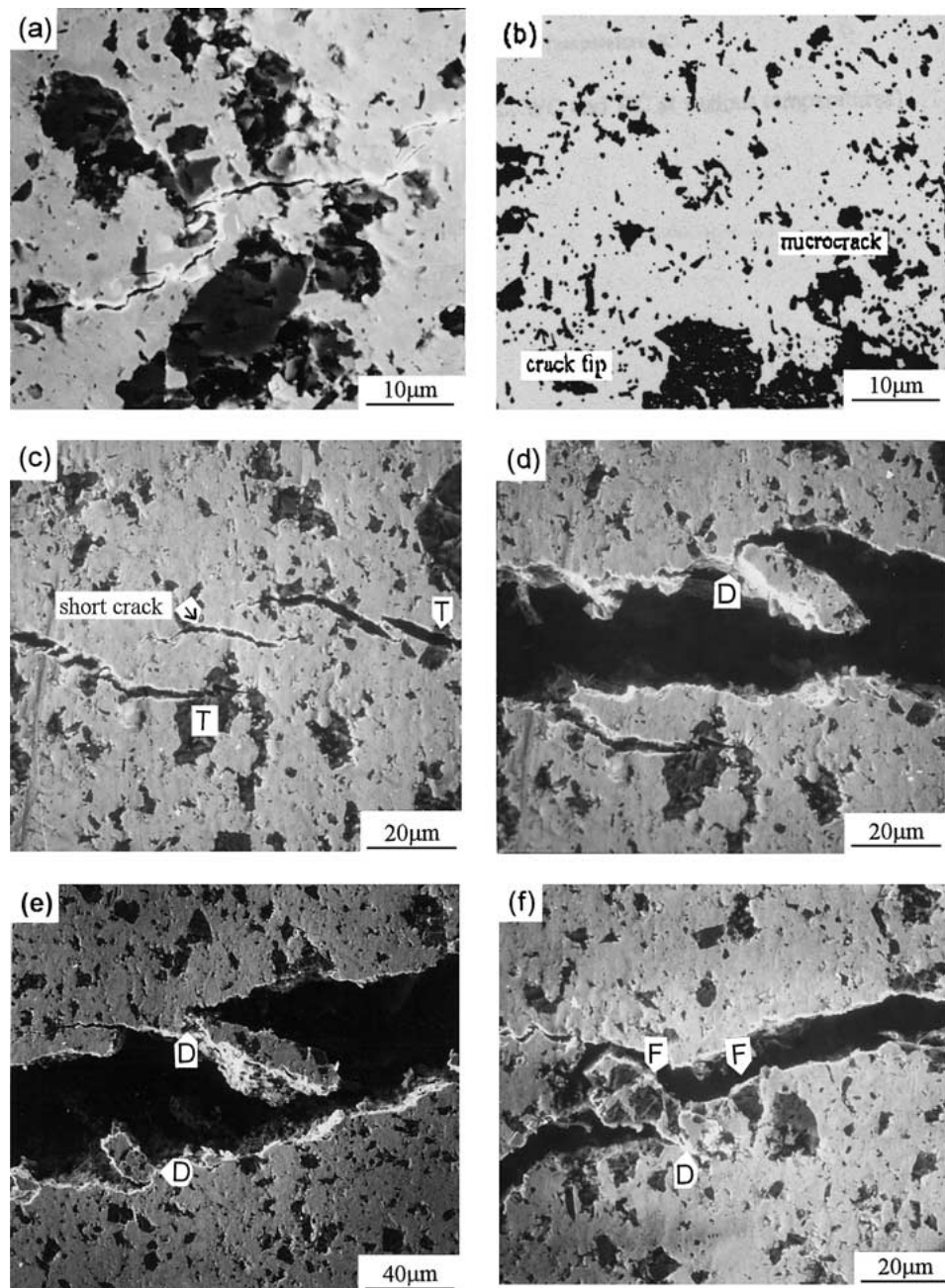
Figure 10 Fracture characteristics of the W-TiC specimens tested at 1000°C: (a) microcracks on the tensile surface; (b) microcrack zone in the vicinity of a crack tip; (c) short cracks; (d) the growth and coalescence of the short cracks in (c); (e) ductile tearing of W matrix; (f) crack propagating in a deflection mode near the W/TiC interface, showing various fracture modes, such as cleavage of TiC particle or TiC cluster (PC), ductile tearing of W matrix (D) and cracking near the W/TiC interface (F).

TiC particles at W grain boundaries create a Zener drag force on the migration of grain boundaries [27].

4. Conclusion

Tungsten matrix composites containing 30 vol% titanium carbide particles have been prepared by vacuum hot pressing at 2000°C. The interdiffusion of Ti and W occurred across the W/TiC interface, resulting in a strong bond. The (Ti, W)C solid solution transition zone formed in the W/TiC interface enhances the strengthening effect of the TiC particles.

The flexural strength of the W/TiC composites is significantly increased by the addition of TiC particles. The flexural strength is 770 MPa and 1155 MPa at room temperature and 1000°C, respectively.

The fracture of the composites at room temperature is brittle. There is metastable crack growth and coalescence during the fracture process at elevated temperature, and the corresponding stress-deflection curves display nonlinear characteristics. The excellent elevated temperature strength of the W-TiC composites is attributed to the strengthening effect of TiC particles on the W matrix. The ductile-brittle transition of the W matrix also plays a very important role on the mechanical behavior. The ductile W matrix makes the strengthening effect of TiC more significant at elevated temperature.

References

1. G. M. SONG, Y. ZHOU, T. C. LEI and Y. J. WANG, *Aerospace Technology* **6** (1997) 43.
2. Z. R. NIE, M. L. ZHOU, Y. CHEN, X. W. FAN, J. X. ZHANG and T. Y. ZUO, *Trans. Nonferrous Metals Soc. China* **9**(1) (1999) 36.
3. S. W. H. YIH and C. T. WANG, "Tungsten-Sources, Metallurgy, Properties and Application" (Plenum Press, New York, 1979).
4. Z. C. CHEN, M. L. ZHOU and T. Y. ZUO, *Scripta Mater* **43** (2000) 291.
5. A. LUO and D. L. JACOBSON, *Int. J. Ref. Ref. Met. & Hard Mater.* **11** (1992) 97.
6. W. D. KLOPP and W. R. WITZKE, *J. Less-Common Met.* **24** (1971) 424.
7. H. M. YUN, *Mater. Sci. Eng.* A **165** (1993) 65.
8. A. LUO, K. S. SHIN and D. L. JACOBSON, *ibid.* **148** (1991) 219.
9. Y. J. WANG, G. M. SONG, Y. ZHOU and T. C. LEI, *Aerospace Mater & Tech.* **28**(28) (1998) 11.
10. Y. KITSUNAI, H. KURISHITA, H. KAYANO, Y. HIRAOKA, T. IGARASHI and T. TAKIDA, *J. Nucl. Mater.* **271/272** (1999) 423.
11. M. MABUCHI, K. OKAMOTO, N. SAITO, M. NAKANISHI, Y. YAMADA, T. ASAHINA and T. IGARASHI, *Mater. Sci. Eng.* A **214** (1996) 174.
12. B. C. MUDDLE, *Metall. Trans.* A **15A** (1984) 1084.
13. K. S. CHURN and R. M. GERMAN, *ibid.* **15A** (1984) 331.
14. H. K. YOON, S. H. LEE, S. J. L. KANG and D. N. YOON, *J. Mater. Sci* **18** (1983) 1374.
15. E. K. STORMS, "The Refactory Carbides" (Academic Press, New York, 1967) p. 3.
16. M. EKROTH, R. FRYKHOLM, M. LINDHOLM and H. O. ANDREN, *J. Agren. Acta Mater.* **48** (2000) 2177.
17. D. L. ZENG, "Power Metallurgy Materials" (Metallurgy Industry Press, Beijing 1989) p. 190.
18. N. LIU, Z. H. HU and K. CUI, *J. Chin. Ceram. Soc.* **25** (1997) 420.
19. T. W. CLYNE and P. J. WITHERS, "An Introduction to Metal Matrix Composites" (Cambridge University Press, New York, 1995).
20. T. Y. KOSOLAPOVA, "Handbook of High Temperature Compounds: Properties, Production, and Application" (Hemisphere Publication Corporation, New York, 1990).
21. Y. S. TOULOUKIAN, R. W. POWELL, C. Y. HO and P. G. KLEMENTS, "Thermophysical Properties of Maters," Vol. 2 (Plenum Press, New York, 1970).
22. Y. J. LIANG and Y. C. CHE, "Handbook of Inorganic Compound of Thermodynamic Data" (Northeastern University Press, Shenyang, 1993).
23. V. N. LIPATNIKOV, A. A. REMPEL and A. I. GUSEV, *Int. J. Refr. Met. & Hard Mater.* **15** (1997) 61.
24. Y. ZHOU, "Ceramic Materials" (Harbin Institute of Technology Press, Harbin, 1995).
25. C. LI and R. M. GERMAN, *Metall. Trans.* A **14A** (1983) 2031.
26. E. RUDY, *J. Less-Common Met.* **33** (1973) 245.
27. D. MCLEAN, "Grain Boundaries in Metals" (Clarendon Press, Oxford, 1957).